

ELECTRICAL INSULATOR COATINGS ON V ALLOYS* J.-H. Park, G. Dragel, and W. D. Cho (Argonne National Laboratory)

OBJECTIVE

Corrosion resistance of structural materials and magnetohydrodynamic (MHD) forces and their influence on thermal hydraulics and corrosion are major concerns in the design of liquid-metal blankets for magnetic fusion reactors. The objective of this study is to develop in situ stable coatings at the liquid-metal/structural-material interface, with emphasis on coatings that can be converted to electrically insulating films to prevent adverse currents that are generated by MHD forces from passing through structural walls.^{1,2}

SUMMARY

Several intermetallic films were applied to V alloys to provide electrical insulation and corrosion resistance. Grain-growth behavior for the V-5Cr-5Ti alloy at 1000°C was investigated to determine the stability of the alloy substrate during coating formation by chemical vapor deposition or metallic vapor processes at 800-850°C. Film layers were examined by optical and scanning electron microscopy and by electron-energy-dispersive and X-ray diffraction analysis; they were also tested for electrical resistivity and corrosion resistance. The results elucidated the nature of the coatings, which provided both electrical insulation and high-temperature corrosion protection.

INTRODUCTION

Corrosion resistance of structural materials and magnetohydrodynamic (MHD) forces and their influence on thermal hydraulics are major concerns in the design of a liquid-metal cooling system for a first-wall/blanket in a magnetic fusion reactor (MFR).^{1,2} Vanadium and V-base alloys (V-Ti or V-Ti-Cr) are leading candidate materials for structural applications in a fusion reactor.³ The objective of this study is to develop stable corrosion-resistant coatings, as well as insulator coatings, at the liquid-metal/structural-material interface. Previous studies focused on in-situ formation of AlN on as-received and prealuminided V alloys in liquid-Li environments.^{4,5} Subsequent work addressed in-situ formation of CaO in a liquid-Li environment because the electrical resistivity of CaO is 10,000 times greater than that of AlN, and because CaO has a high thermodynamic stability in liquid Li among the available insulator candidates (i.e., CaO, Y₂O₃, BeO, MgO, MgAl₂O₄, Y₃Al₂O₁₂, etc.).⁵⁻⁷ The coatings should be formable on various shapes, such as the inside of tubes or irregular shapes to prevent adverse currents that are generated by MHD forces from passing through the structural walls. The coatings could also improve general corrosion resistance and act as a diffusion barrier for hydrogen isotopes, i.e., deuterium and tritium.

DEVELOPMENT OF INSULATOR COATINGS

Several experimental steps were employed to develop insulator coatings on V-base alloys, namely, (a) screening of selected electrical insulators in liquid Li based on thermodynamic stability, electrical resistivity, coefficients of thermal expansion (CTE), and diffusion coefficients of cations and anions within the coating layer; (b) liquid-Li compatibility tests for candidate electrical insulators;^{5,6} and (c) methods of in-situ fabrication of intermetallic coatings in liquid Li by conversion of an intermetallic layer to an electrical insulator coating in a controlled environment. Failure (cracking or spallation) and self-healing characteristics of the coating layer are also important in MFR applications.

* Work supported by U.S. Department of Energy, Office of Fusion Energy Research, under Contract W-31-109-Eng-38.

Solid-State Interactions: Bonding Of AlN And Metal/Alloy Substrates

Solid-state interactions between AlN and several metals and alloys (viz., V, V-5%Cr-5%Ti, Ti, and Type 316 stainless steel) were investigated. Sintered discs of Y₂O₃-enriched AlN (12.7 x 50 x 9 mm) were obtained from the Ceramics Section at Argonne National Laboratory. Inductively-coupled-plasma (ICP) spectrochemical analysis of the AlN samples indicated the following composition (in wt.%): As <0.05, Ba = 0.005, Be <0.001, Ca = 0.54, Co <0.002, Cr <0.002, Cu = 0.006, Fe = 0.015, Y = 3.77, Y₂O₃ = 4.79, Mg = 0.004, Mn <0.001, Ni = 0.002, Pb <0.02, Sb <0.05, Sn <0.02, Sr <0.001, Ti = 0.022, V <0.002, Zn <0.002, Zr <0.002, and Te <0.05. The discs were cut into pieces measuring ≈12.7 x 12.7 x 2.7 mm, ground flat on Struers 4000 silicon carbide paper, and then ultrasonically cleaned in isopropyl alcohol. A disc of each metal or alloy was placed between two AlN discs and the entire stack was placed in a furnace. A compressive force was applied to the stack by placing a 120° three-spring-loaded alumina rod on the top of the stack. A detailed description of the apparatus is provided in Ref. 7. The AlN/alloy stack was annealed in a furnace at 900°C for 129 h in flowing 3%H₂-N₂. After cooling, the specimen stack was examined for indications of strong bonding between AlN and alloy substrates. Interfaces between the alloys and AlN were examined by scanning electron microscopy and energy dispersive spectroscopy to determine diffusion profiles of various elements. Results for the diffusion couples are given below.

V/AlN V diffused into AlN, but a bond was not formed and VN was not detected. The absence of a good bond and no interdiffusion of N are not conducive to the development of an adherent coating by a high-temperature process. In this case, a low-temperature physical vapor deposition (PVD) technique could be tried, but if the operating temperature increases or the service time is very long, the base metal, V, could be degraded by formation of vacancies at the metal/AlN interface, grain boundaries, and dislocations. Eventually, vacancies could coagulate to form voids within the V substrate and possibly lead to debonding of the coating.

Ti/AlN Ti did not bond with AlN but a thin layer formed at the Ti/AlN interface. This is indicative of a Ti_xN_y phase, and some diffusion of N into Ti was evident. Bonding of AlN/Ti_xN_y exhibited sintering-like behavior; however, Ti_xN_y was detached from Ti in some areas, which indicates outward diffusion of Ti during the formation of Ti_xN_y. These processes are shown in Fig. 1.

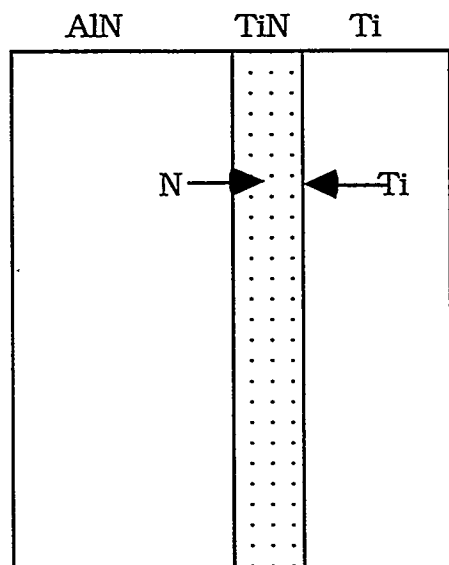


Figure 1.

Schematic diagram of solid-state reaction steps at Ti/AlN interface:

1) $\text{AlN} + \text{Ti} = \text{Ti}_x\text{N}_y + \text{AlN}_{1-d}$: initial reaction

(x and $y \approx 1$, $d \ll 1$)

2) $\text{AlN}/\text{AlN}_{1-d}/\text{Ti}_x\text{N}_y/\text{Ti} \rightleftharpoons \text{Ti}_x\text{N}_y$: layer grows by N diffusion from AlN to Ti

3) $\text{AlN}/\text{AlN}_{1-d}/\text{Ti}_x\text{N}_y/\text{Ti}$:

Ti and N interdiffusion and growth occurs in Ti_xN_y layer; TiN/Ti interface bond weakens due to outward diffusion of Ti

V-5Cr-5Ti/AlN Neither V, Ti, nor the V alloy bonded with AlN. Minimal information was obtained because no bonding occurred. Coarsening of grains in V-5Cr-5Ti at the alloy/AlN interface was observed, and may have been accelerated by applied pressure.

Type 316 stainless steel/AlN Reaction occurred between a thin oxide scale, Cr_2O_3 , on Type 316 stainless steel and AlN to form Al-Cr-O. AlN particles were found on the surface of the steel, which suggests that a strong bond could be produced in this couple. Dissolved oxygen in the steel transferred to the surface and reacted with AlN to form Al-O-N at the interface. The predicted products from this diffusion couple are AlN/Al-O-N/Al-Cr-O/SS after long-term exposure. Strong bond formation between the Type 316 stainless steel/AlN interface was observed. This couple is applicable to the development of insulator coatings because the ohmic resistance of Al-O-N phase was higher than expected. In the same vein, we may pursue the interaction of oxygen-charged V-5Cr-5Ti alloys with AlN to produce a V-5Cr-5Ti-(O)/Al-O-N/AlN couple, which may also reveal enhanced ohmic resistance. Preparation of oxygen-charged V-5Cr-5Ti was described previously.⁸

Diffusion Approach to In-Situ Formation of Insulator Coatings in Liquid Li

Ionic diffusion (cation, anion or both) within the coating must be considered during formation of insulator coatings, as should long-term exposure of these coatings in liquid-Li environments.

Outward cation or anion diffusion from alloys or ceramic substrates In this case, a metal ion (cation) or anion leaves the substrate and migrates to the scale/liquid-metal interface, and a vacancy may be produced at a grain boundary, dislocation, or other active defect area within the substrate (Fig. 2). The consequences of predominantly outward-diffusing species at the metal/coating interface are vacancy formation and coalescence (void formation) near the interface, and reduction in the bond strength between coating/substrate. However, if the chemical potential gradient at the coating and substrate is relatively small at elevated temperatures, void formation may not occur. In general, outward cation or anion diffusion from alloys or ceramic substrates should be avoided.

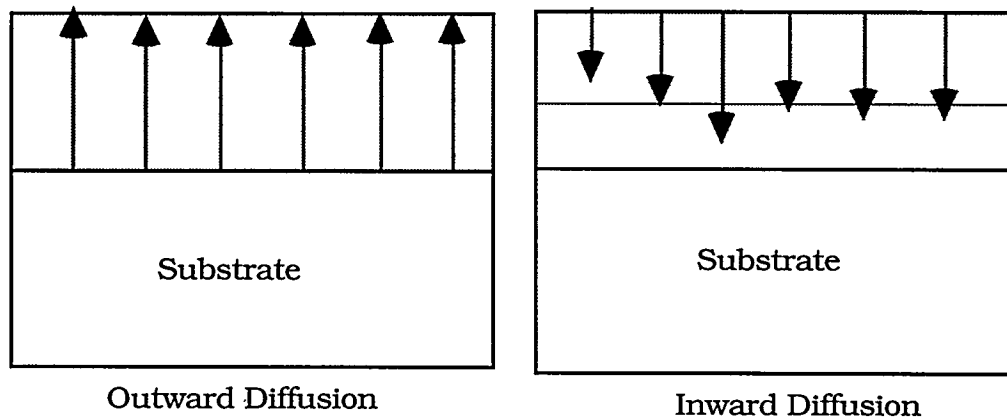


Figure 2. Formation of coating layers by different diffusion profiles

Inward diffusion via insulator layer If anions of O, N, or C within the coating layer diffuse inward toward the alloy, insulator-layer growth occurs at the alloy/coating interface. However, diffusion of cations from metal atoms in the liquid environment must also be considered.

Grain-Growth Behavior of V-5%Cr-5%Ti

In coatings produced by high-temperature processes, such as chemical vapor deposition (CVD) or thermally grown layers, grain growth and changes in morphology of the alloy influence the coating properties.⁸ Even though the CTE of the substrate and coating layer are similar in magnitude, adherent coatings may not form because of inadequate stabilization of alloy substrate. This is more prevalent in the case of brittle ceramic or intermetallic coatings on metallic substrates because of diffusion-related phenomena in the metal (e.g., grain growth) rather than in the ceramic at high processing temperatures. For high-temperature alloys, viable coatings require alloy stabilization before coating application;⁹ otherwise, the coating layers tend to spall during high-temperature operation because of grain growth or other morphological changes. In the case of Fe-Cr steels, a small amount of Y (≈ 0.3 wt.%) in the alloy inhibits grain growth.⁹

The V-5%Cr-5%Ti specimens were wrapped in Ta foil, sealed in quartz capsules in vacuo to avoid Si or O contamination, and annealed for 0.3–61.3 h at 1000°C. Figures 3 and 4, respectively, show grain morphology and change in grain diameter of V-5%Cr-5%Ti as a function of time. At 1000°C, grain growth decreases rapidly after ≈ 2.5 h; the grain size of a specimen annealed for 24 h is almost the same as the one annealed for 2.5 h. The increase in grain size, Δd , was 7 μm for an initial average grain size of 7 μm . Grain-growth behavior at 1000°C in terms of $\log \Delta d$ versus $\log t$ can be represented by

$$\log \Delta d = 0.58 + \log t^{0.53}, \quad (1)$$

where the ≈ 0.5 exponent of time is indicative of a diffusion mechanism. Based on these results, we expect that grain growth will not have a significant effect on high-temperature coatings that are applied by processes such as CVD, pack cementation, or PVD.

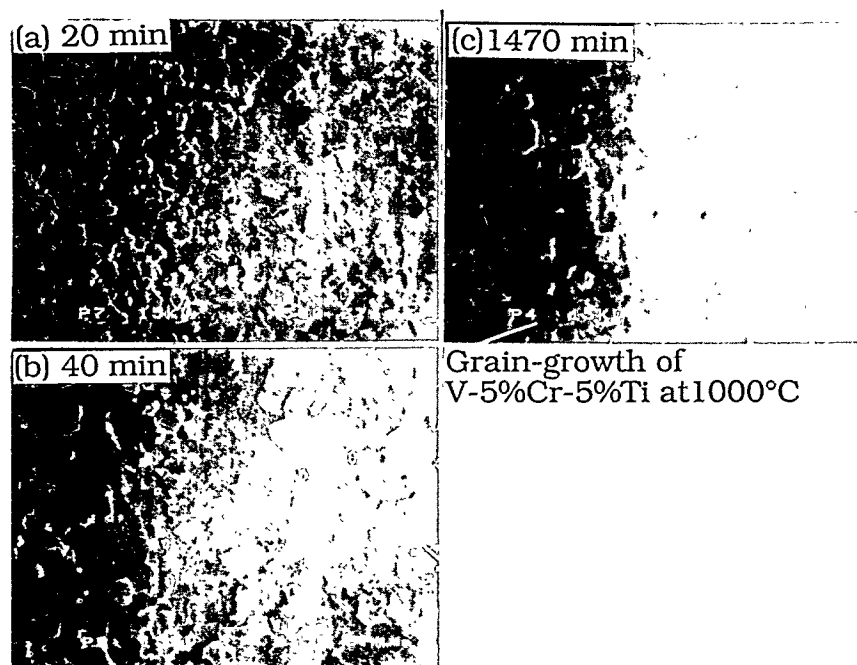


Figure 3. SEM photomicrographs of V-5%Cr-5%Ti specimens after annealing for 20, 40, and 1470 min. at 1000°C in grain-growth experiments

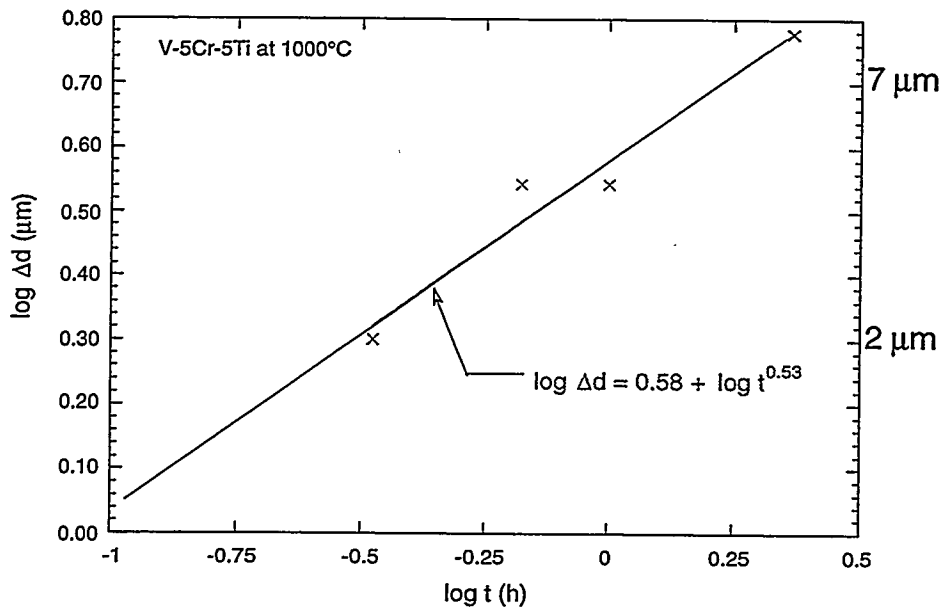


Figure 4. Increase in grain size (Δd , μm) as a function of time at 1000°C for V-5%Cr-5%Ti specimens from as-received value $7 \mu\text{m}$

Formation of Intermetallic Coatings

Various intermetallic and insulator layers were developed by different methods, namely, CVD, high-temperature PVD, ion-beam-assisted deposition (IBAD), and exposure of specimens to liquid Li containing dissolved metallic solutes (Al, Be, Mg, Si, Ca, Pt, Y, and Cr) to form coatings by chemical reaction with constituents in various metals and alloys (Ti, V-5Cr-5Ti, V-Ti, Types of 304 and 316 stainless steel, Fe-25Cr with 0.3Y or 6Al). Most of the solutes in Li were chosen on the basis of thermodynamic stability of their metal oxides or nitrides in Li, as well as on results of compatibility screening tests for ceramic materials in Li.

Chemical Vapor Deposition

Aluminide and AlN coatings Aluminide coatings that form on structural alloys during exposure to liquid Li that contained dissolved Al suggest a means for producing stable electrical insulator layers, such as AlN, by subsequent nitration of the intermetallic layer in the liquid-metal environment.⁷ The formation of several aluminides (V_xAl_y) that contain >40–50 at.% Al on V-base alloys can be predicted from the V-Al phase diagram.^{10,11} These phase relationships are the basis for the formation of aluminide coatings on V and its alloys. Aluminide coatings were produced on the alloys by CVD at $800\text{--}850^\circ\text{C}$ with trimethyl aluminum $(\text{CH}_3)_3\text{Al}$ as the source of Al to be diffused/reacted on the sample surfaces. In this study, atmospheric-pressure CVD was used because of its utility for engineering applications. Figure 5 is a schematic diagram of the CVD apparatus. The $(\text{CH}_3)_3\text{Al}$ vapor was aspirated by a 3% $\text{H}_2\text{--Ar}$ carrier gas with impurity oxygen and carried to the high-temperature zone via a Ta tube, where the vapor decomposed and reacted with the specimens. The reaction for the formation of aluminides is



and the ΔG° range for the reaction is -4 to -5 kcal/mole (Fig. 6). This process was followed by mixing NH_3 into the gas stream to convert the aluminide to an AlN coating according to the reaction

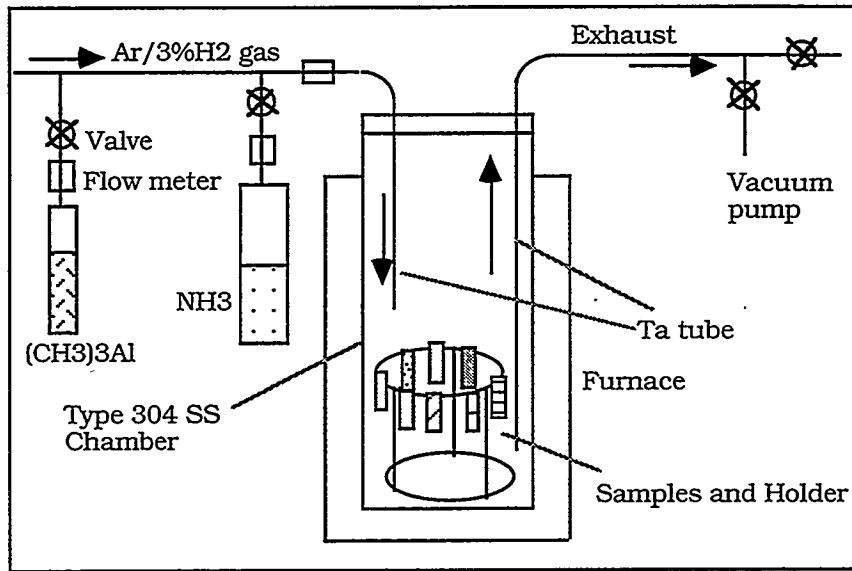


Figure 5. Schematic diagram of CVD apparatus

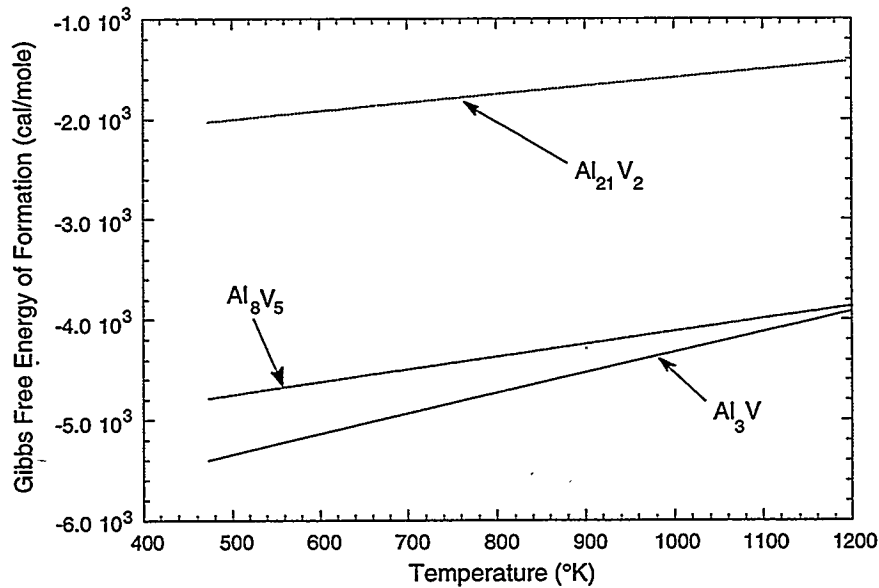


Figure 6. Gibbs free energy of formation for various intermetallic compounds in Al-V system as a function of temperature



where \underline{N} represents nitrogen activity in the gas phase or dissolved in liquid Li. The free energy of formation of AlN is -45.94 kcal/mole; therefore, the ΔG° for the reaction in Eq. (3) is -40.94 kcal/mole at 700 K. This reaction will occur spontaneously, and the rate-determining step will be ionic diffusion through the nitride layer. Residual V formed during the reaction will either redistribute within Al_3V , or AlN will become enriched in V, depending on the direction of V diffusion and the thermodynamic stability

of V_2N near the Al_3V/AlN interface. Because of the high thermodynamic stability of TiN , formation of this phase on aluminided $V-5\%Cr-5\%Ti$ is also a possibility.*

Figure 7 (a) is an SEM photomicrograph of an intermetallic V aluminide coating on a $V-5Cr-5Ti$ substrate. The chemical composition of the coating surface, by EDS is as follows:

Al	61.34 at.%	(45.72 wt.%)
V	33.57 at.%	(47.23 wt.%)
Cr	2.72 at.%	(3.91 wt.%)
Ti	2.37 at.%	(3.13 wt.%)

Based on these compositions and the on $V-Al$ binary phase diagram, the composition of the intermetallic phase at the surface lies between Al_3V and Al_8V_5 . When we consider the free energy of formation of $Al-V$ intermetallic phases (Fig. 6), the Al_3V phase should form because of its greater stability, but at high temperatures ($850^\circ C$, $1123 K$) a mixture of Al_3V and Al_8V_5 could arise because of the similar magnitudes of the free energies of formation. However, if Al concentration is too low (e.g., <40 at.%), $V-Al$ intermetallic phases will not form at the surface and Al will only diffuse into the bcc sublattice of V according to the phase diagram. Based on our previous work,¹² Al_3V was prevalent on various $V-Cr-Ti$ alloys.

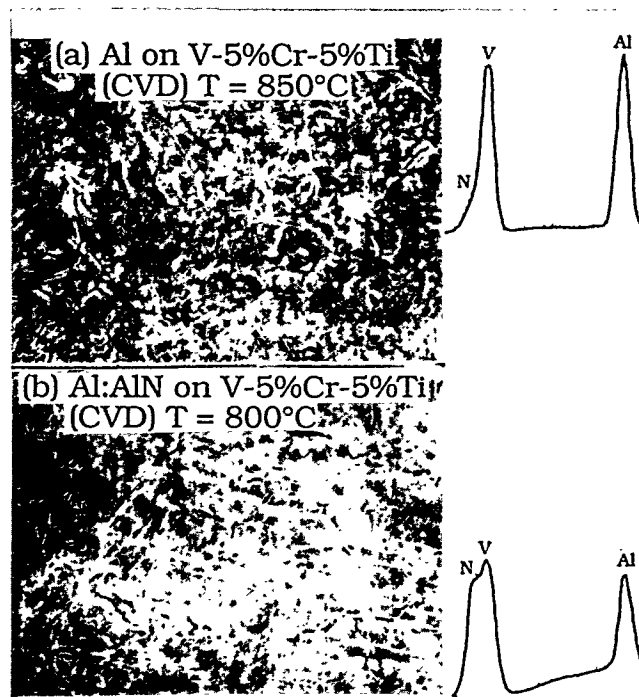


Figure 7. SEM photomicrographs and EDS spectra of (a) aluminide and (b) Al/AlN coating deposited by CVD on $V-5Cr-5Ti$ specimens at two temperatures

* When we exposed prealuminide $V-5Cr-5Ti$ to liquid Li containing 100-200 ppm N , TiN grew outward between the aluminide grains.

Figure 7 (a) also shows the EDS spectra of an aluminide surface on V-5%Cr-5%Ti at 850°C, and Fig. 7 (b) shows similar information for an AlN surface formed at 800°C. The Ta tube that carried the gas into the high-temperature zone was also analyzed. Figure 8 shows the Ta-Al intermetallic and AlN coatings on the inner surface of the tube. CVD, in which AlCl₃/NH₃ is the source of Al, may not be applicable to many materials because of Cl-induced corrosion. An SEM photomicrograph of a CVD coating on V-5%Cr-5%Ti at 850°C showed total spallation of deposited AlN when AlCl₃ was used. When V chloride compounds form during the coating process, they tend to spall and prevent the formation of an adherent AlN layer at the surface.

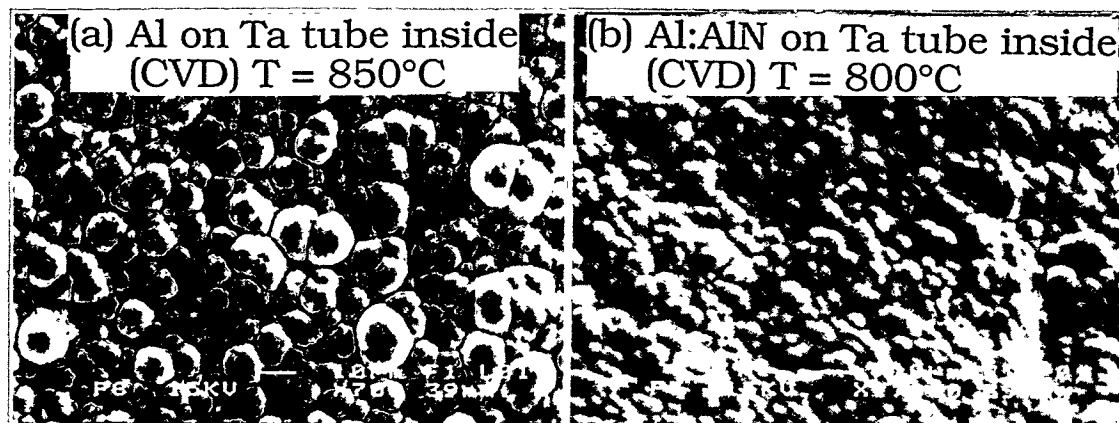


Figure 8. SEM photomicrograph of (a) aluminide, and (b) Al/AlN coating on inside surface of Ta tubes

Al₂O₃ Coatings on Stainless Steels in Air

Low rates of elemental diffusion and electron transport in Al₂O₃ are desirable properties for high-temperature corrosion-resistant coatings. However, benefits from these properties for high-temperature coating applications are rather limited because crack-free Al₂O₃ coatings are extremely difficult to fabricate. In this study, we have had some success in forming Al₂O₃ coatings on Types 304 and 316 stainless steel. Coatings were produced by growing an intermetallic aluminide layer (FeAl) on the steels in liquid Li containing 4–5 wt.% dissolved Al, followed by oxidation of the aluminide layer in air at 1000°C. To determine the minimum required Al content of the steel to form an Al₂O₃ coating layer, samples of an aluminided steel tube were sectioned and polished and an Al depth profile was measured by EDS (detection limit of ≈1 at.%). After oxidation, an Al spectrum from EDS indicated a continuous Al₂O₃ coating layer had formed.

Based on our previous experience, most Al₂O₃ coating layers formed on Fe–Cr–Al alloys contained numerous cracks, mainly due to mismatch of the CTEs (≈8 × 10⁻⁶/K for Al₂O₃ and ≈17 × 10⁻⁶/K for stainless steel). We believe that Li (130 ppm) in the aluminide layer that formed in liquid-Li containing Al plays a role in accommodating thermal stresses during Al₂O₃ growth and cooling because of fast diffusion of Li⁺ ions due to their small size.

High-Temperature Metallic Vapor Deposition of MgO Coating

MgO and CaO MgO is another potential candidate for an insulator coating in a liquid-Li blanket of an MFR. An MgO coating could be applied to various components by vapor deposition because metallic Mg has a high vapor pressure at elevated temperatures. This coating method was investigated with an apparatus similar to that shown in Fig. 5. Mg vapor was generated in a high-temperature Knudsen cell

located at the bottom of the stainless steel chamber, which provided a homogeneous source of Mg vapor. Mg was contained in a tungsten or Type 304 stainless steel boat and covered with a plate that contained an ≈ 1.5 -mm-diameter pin hole. Sublimation of Mg in a relatively low vacuum of 10^{-3} - 10^{-4} torr, in which O_2 was present as an impurity, enabled the formation of MgO clusters by oxidation of Mg vapor inside the chamber. After coating the V-5Cr-5Ti specimens at 800°C , the system was cooled to room temperature by purging with Ar (99.999%). The ohmic resistance of the coatings was measured at room temperature and the coatings were evaluated by SEM/EDS. Figure 9 a shows a typical MgO coating on V-5Cr-5Ti; its EDS spectrum is shown in Fig. 9 b. The measured two-point contact resistance at room temperature is $>10^{12} \Omega$. This technique was also applied to the CaO coating, which showed a trend similar to that observed with MgO. We found that this technique could be extended to other oxides, e.g., BeO , MgAl_2O_4 , $\text{Y}_3\text{Al}_2\text{O}_{12}$, etc.

(a) Mg:MgO on V-5%Cr-5%Ti
(PVD) $T = 800^\circ\text{C}$

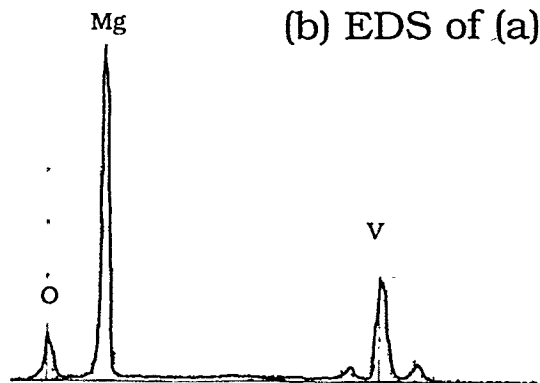
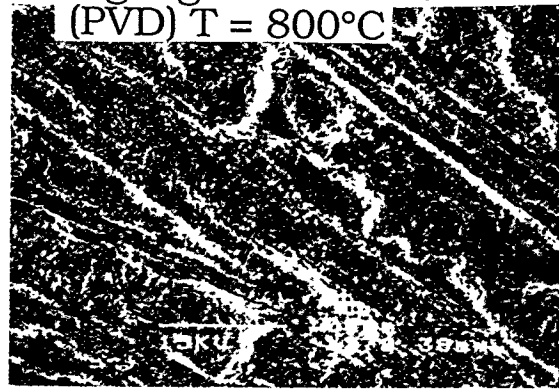


Figure 9. (a) Photomicrograph of MgO coating on V-5Cr-5Ti; (b) EDS of coating shown in (a)

CONCLUSIONS

High-temperature couples between AlN and V alloys, Ti, and Types 304 and 316 stainless steel showed different interface bonding behavior. Basically, V alloy/AlN couples did not bond. In the case of Ti/AlN, TiN formed at the interface, but the bonding strength was too low and separation occurred at the Ti/TiN interface. Strong bonds were obtained between AlN and the stainless steels, but mismatch in the thermal expansion coefficients caused fracture in the relatively thick AlN layer above the alloy/AlN interface.

Intermetallic films were prepared on V alloys and Types 304 and 316 stainless steel by chemical vapor deposition, high-temperature metallic vapor deposition, and liquid-metal processing in the temperature range of 800–850°C. The films were examined by optical and scanning electron microscopy and by electron-energy-dispersive and X-ray diffraction analysis. Aluminide films containing >45 wt.% Al and AlN were produced on V alloys by CVD. The aluminide films on Types 304 and 316 stainless steel were converted to Al₂O₃ by oxidation in air at high temperature. The results elucidated the nature of the coatings, which provided both electrical insulation and high-temperature corrosion protection.

FUTURE WORK

Several other ternary oxides systems (e.g., spinel; MgAl₂O₄, and/or garnet; Y₃Al₂O₁₂) will be fabricated by either a CVD or an in-situ liquid-Li process, and the films will be tested for the liquid-Li compatibility and in-situ electrical resistivity.

REFERENCES

1. C. C. Baker et al., *Tokamak Power System Studies FY 1985*, Argonne National Laboratory Report ANL/FPP-85-2 (1985).
2. T. Kammash, *Fusion Reactor Physics*, Chapter 15, Ann Arbor Science Pub. Inc., Ann Arbor, MI (1975), pp. 405-439.
3. R. F. Mattas, B. A. Loomis, and D. L. Smith, *Vanadium Alloys for Fusion Reactor Applications*, JOM, 44(8), 26 (1992).
4. J.-H. Park, T. Domenico, G. Dragel, and R. W. Clark, *Development of Electrical Insulator Coatings for Fusion Power Applications*, Proc. 3rd Intl. Symp. on Fusion Nuclear Technology (ISFNT), June 27-July 1, 1994, Los Angeles, CA.
5. J.-H. Park and G. Dragel, *Development of Aluminide Coatings on Vanadium-Base Alloys in Liquid Lithium*, Fusion Reactor Materials Semiannual Progress Report for the Period Ending March 31, 1993, DOE/ER-0313/14, pp. 405-410 (1993).
6. R. J. Lauf and J. H. DeVan, *Evaluation of Ceramic Insulator for Lithium Electrochemical Reduction Cells*, J. Electrochem. Soc., 139, 2087-2091 (1992).
7. J.-H. Park and G. Dragel, *Development of Electrical-Insulator Coatings: In-situ Electrical Resistance Measurements on V-5%Cr-5%Ti in Liquid Lithium*, Fusion Reactor Materials Semiannual Progress Report for the Period Ending September 30, 1993, DOE/ER-0313/15 (1993).
8. J.-H. Park, *Surface Modification of High-Temperature Alloys*, Mater. Technol., 9, 9/10 (1994).
9. J.-H. Park, *Surface Modification of High-Temperature Alloys*, The Electrochem. Soc. 186th Meeting, The D. Douglass Symp. on High-Temperature Corrosion, Oct. 9-14, 1994, Miami, FL.
10. M. Hansen, *Constitution of Binary Alloys*, McGraw-Hill, New York (1958).
11. F. A. Shunk, *Constitution of Binary Alloys, Second Supplement*, McGraw-Hill, New York (1969).
12. J.-H. Park, *Intermetallic and Electrical Insulator Coatings on High-Temperature Alloys in Liquid Lithium Environments*, Proc. Symp. on High-Temperature Coatings-I, TMS Fall Meeting, Oct. 2-6, 1994, Rosemont, IL.